PERGAMON

Journal of Asian Earth Sciences 21 (2003) 743–753

Journal of Asian Earth Sciences

www.elsevier.com/locate/jseaes

2.9, 2.36, and 1.96 Ga zircons in orthogneiss south of the Red River shear zone in Viet Nam: evidence from SHRIMP U–Pb dating and tectonothermal implications

Tran Ngoc Nam[a,*], Mitsuhiro Toriumi[b], Yuji Sano[c], Kentaro Terada[c], Ta Trong Thang[d]

[a]*Department of Geosciences, Hue University of Science, 77-Nguyen Hue, Hue City, Viet Nam*
[b]*Graduate School of Frontier Sciences, the University of Tokyo, 7-3-1 Hongo, Tokyo 113-0033, Japan*
[c]*Department of Earth and Planetary Sciences, Hiroshima University, Kagamiyama 1-3, Higashi-Hiroshima 739-8526, Japan*
[d]*Department of Geology, Hanoi National University, 334-Nguyen Trai, Hanoi, Viet Nam*

Received 1 May 2001; revised 19 April 2002; accepted 21 May 2002

Abstract

Orthogneissic rocks coexisting with migmatites and containing small amphibolite lenses are exposed in the center of the metamorphic belt which runs parallel to the Day Nui Con Voi–Red River shear zone in northern Viet Nam. The orthogneiss complex has given some radiogenic dates of Early Proterozoic and Late Archean, which are the oldest ages ever registered for the Southeast Asian continent. Zircon grains separated from three samples of the orthogneiss complex have been dated to establish the protolith age and the timing of high-grade tectonothermal events in the complex. Sixty-five SHRIMP U–Th–Pb analyses of these zircons define three age groups of 2.84–2.91, 2.36, and 1.96 Ga. The age groups correspond to three periods of zircon generation. The oldest ~2.9 Ga cores indicate a minimum age for the protolith of the orthogneiss complex. Two younger generations (including ~2.36 Ga outer-cores and ~1.96 Ga rims) probably grew during later high-grade tectono-metamorphic events, which were previously suggested by K–Ar and $^{40}Ar/^{39}Ar$ cooling ages of ~2.0 Ga for synkinematic hornblendes. An early thermal history of the orthogneiss complex has been constrained, including a primary magma-crystallization stage starting at ~2.9 Ga, followed by two Early Proterozoic (~2.36 and ~1.96 Ga) high-grade tectonothermal events.

The ca. 2.9 Ga protolith age of the orthogneiss complex documented in this study provides new convincing evidence for the presence of Archean rocks in Indochina, and clearly indicates that the crustal evolution of northern Viet Nam started as early as Late Archean time.
© 2003 Elsevier Science Ltd. All rights reserved.

Keywords: SHRIMP U–Pb dating; Zircon geochronology; Archean; Red River shear zone; Viet Nam; Indochina

1. Introduction

The Indochina peninsula is recognized as an 'ideal natural laboratory' for scientists studying the geological consequences of collision/extrusion tectonics (Tapponnier et al., 1986), and has recently attracted much attention from the international community. As a result, the quality and quantity of geological studies of Indochina and of the adjacent area have increased dramatically in the last decade, improving our understanding of the tectonothermal events in the region. Recent geochronological studies, mostly by K–Ar and $^{40}Ar/^{39}Ar$ methods, have revealed the occurrence of three tectonothermal episodes, including the Triassic Indosinian, Late Jurassic–Early Cretaceous (Maluski et al., 1995, 1997, 2001; Lepvrier et al., 1997; Nam, 1998; Carter et al., 2001), and Tertiary (Jolivet et al., 1999; Tapponnier et al., 1990; Schärer et al., 1990, 1994; Leloup et al., 1995; Harrison et al., 1996; Nam et al., 1998; Wang et al., 1998, 2000). However, pre-Indosinian tectonothermal events are still poorly documented, and geochronological data for high-temperature stages of the tectonothermal evolution remain scarce.

High-grade metamorphic terrains in Viet Nam are well exposed in the Kontum massif (KT; Fig. 1(a)) and in the Red River fault zone area (RRFZ; Fig. 1(a)). The central part of the Kontum massif is mainly composed of orthopyroxene granulites and associated rocks, which petrologically are similar to those of the Eastern Ghats (India) and East Antarctica. These granulites were previously interpreted to

* Corresponding author. Tel.: +84-54-823837; fax: +84-54-824901.
E-mail address: nam.hue@dng.vnn.vn (T.N. Nam).

1367-9120/03/$ - see front matter © 2003 Elsevier Science Ltd. All rights reserved.
PII: S1367-9120(02)00089-5

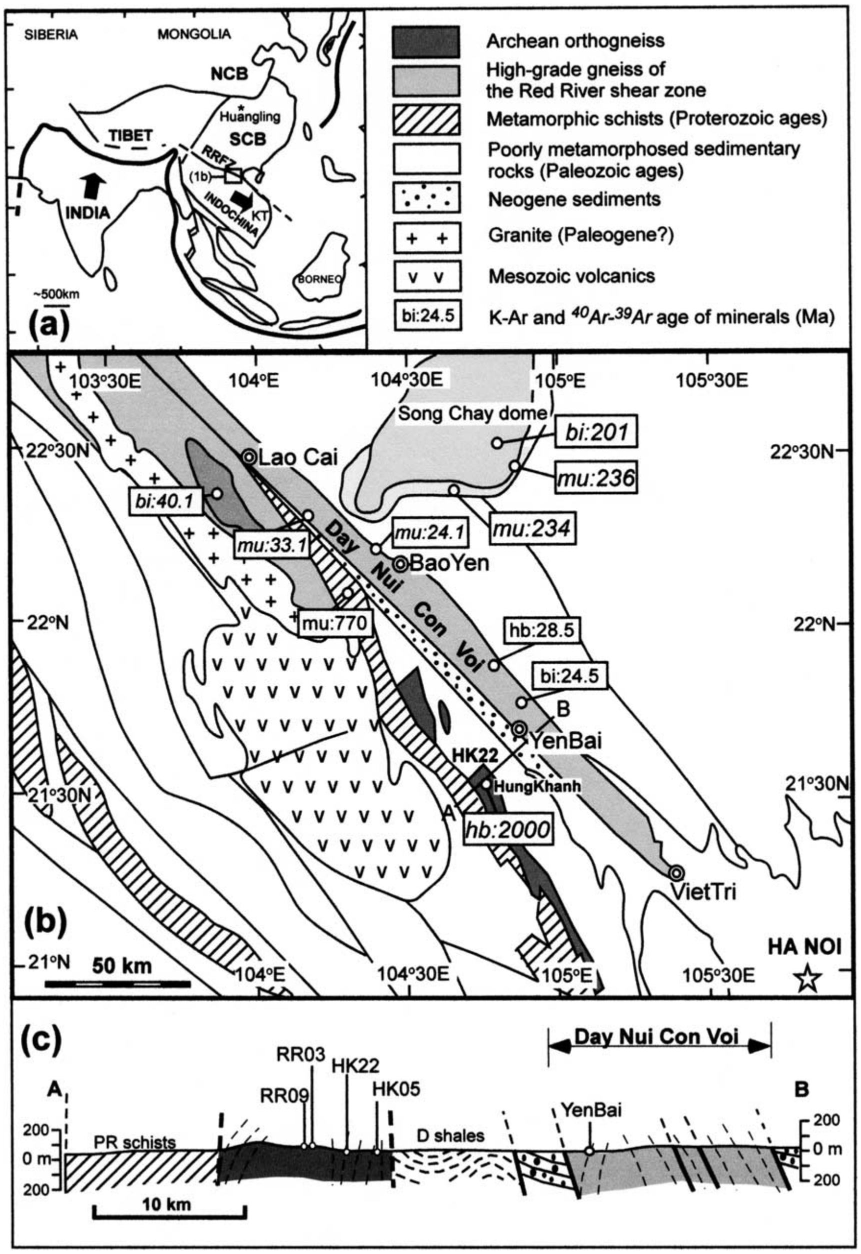

Fig. 1. (a) The Red River fault zone in Viet Nam, China, (b) geological sketch map around the Day Nui Con Voi–Red River shear zone, and (c) cross-section through the Day Nui Con Voi and pre-Mesozoic metamorphic belt, northern Viet Nam. Abbreviations: KT, Kontum massif; NCB, North China Block; RRFZ, Red River fault zone; SCB, South China Block. K/Ar ages (Ma) of biotite (bi), muscovite (mu) and hornblende (hb) (in boxes) from Nam et al. (1998, 2000b), and Ar/Ar ages (Ma) of minerals in *italic characters* (in boxes) from Maluski et al. (2001). Locations of samples HK22, RR03, and RR09 (this study) and of HK05 (Nam et al., 1998) are shown.

be Archean and were thought to be the oldest rocks of the Indochina craton (Hai, 1986; Hutchison, 1989), but recent SHRIMP U–Pb zircon dating has shown that high-grade granulite facies metamorphism occurred during Indosinian times (ca. 254 Ma) (Nam et al., 2001; Carter et al., 2001). The protolith age of these granulites is likely to be Mid-Proterozoic (ca. 1.4 Ga) according to the age obtained on a zircon core (Nam et al., 2001). On the other hand, high-grade gneiss massifs of the Red River shear zone, that were metamorphosed under amphibolite facies conditions of $\sim 700\,^{\circ}C$ and 0.65 ± 0.15 GPa (Nam et al., 1998), have previously given a wide range of ages from Miocene (12 Ma) to Precambrian (1700 Ma) (see Tapponnier et al. (1990)), suggesting a complicated tectonothermal history. Schärer et al. (1990, 1994) and Zhang and Schärer (1999) showed that U–Pb ages on monazite, xenotime, zircon and titanite from late syntectonic leucogranitic veins in the Red River shear zone in Yunnan, China (the Diancang Shan and Ailao Shan massifs) cluster at 22–33 Ma, indicating the crystallization ages of the veins. Some inherited components in zircon, giving upper-intercept ages of 1.2–1.6 Ga, provide evidence for the presence of Proterozoic crust in this region. $^{40}Ar/^{39}Ar$ and K–Ar dating of hornblende, mica and K-feldspar yielded cooling ages of ca. 20–30 Ma for high-grade gneissic rocks from the Red River shear zone including the Xuelong Shan, Diancang Shan, Ailao Shan massifs in Yunnan (China) (Leloup et al., 1995; Harrison et al., 1996), and the Day Nui Con Voi in Viet Nam (Fig. 1(b)) (Nam et al., 1998; Wang et al., 1998, 2000; Maluski et al., 2001). These massifs were interpreted to have formed during the Tertiary India–Asia collision (Tapponnier et al., 1990; Leloup et al., 1995).

Bodet and Schärer (2000) dated zircons and baddeleyites from four large rivers in the Indochina continent by the U–Pb method. Their analyses reveal ages younger than 2.5 Ga for 235 single zircon and baddeleyite grains, leading these authors to argue for the absence of Archean crust in these rivers' drainage-area. Most recently, Lan et al. (2001) reported Archean Nd model ages of 3.4–3.1 Ga and TIMS U–Pb zircon dates of 2.8–2.5 Ga for the orthogneiss complex south of the Day Nui Con Voi, whose synkinematic hornblendes were previously dated at ca. 2000 Ma by K–Ar and $^{40}Ar/^{39}Ar$ single grain dating using a laser step-heating technique (Nam et al., 1998, 2000a). SHRIMP U–Pb zircon geochronology of the orthogneiss complex will help to identify precisely the old ages and to characterize possible high-grade events.

2. Geological setting

The Day Nui Con Voi–Red River shear zone in northern Viet Nam appears as a narrow (< 10 km) and elongated (~250 km) metamorphic zone trending from NW to SE (Fig. 1(a)). The zone consists mainly of biotite–sillimanite–garnet gneiss, garnet–biotite gneiss, garnet-bearing two-mica schists and migmatites, which are associated with mylonite bands and amphibolite and marble lenses. Geothermobarometry using coexisting garnet–biotite–plagioclase of sillimanite-bearing gneisses, and garnet–hornblende–plagioclase–quartz of amphibolite suggested that the peak metamorphism occurred under amphibolite facies conditions of 690 ± 50 °C and 0.65 ± 0.15 GPa (Nam et al., 1998). Recent K/Ar and $^{40}Ar/^{39}Ar$ analyses of hornblende and biotite gave cooling ages of 20–30 Ma (Harrison et al., 1996; Nam et al., 1998; Wang et al., 1998; Maluski et al., 2001), although the Day Nui Con Voi has long been traditionally regarded as Early Proterozoic (Tri, 1977).

The pre-Mesozoic belt, running parallel and to the south of the Day Nui Con Voi, is composed mainly of orthogneisses coexisting with migmatites and small bodies of amphibolite in the center, almandine-bearing mica schists in the southwest side, and Devonian shale-sandstone in the northern flank. The rock association of orthogneisses and migmatites in the center part indicates a high-grade of metamorphism. The orthogneisses, exposed as 7–15 km wide, 50–70 km long, NW trending bodies have been severely deformed (see Nam et al. (1998) for more details). The orthogneisses commonly have the mineral assemblage of quartz, plagioclase, K-feldspar, hornblende, biotite and epidote, indicating epidote–amphibolite facies metamorphic conditions. In the orthogneiss zone, small amphibolite lenses elongated parallel to the belt are locally present. Synkinematic hornblendes from the orthogneiss and amphibolite were dated at ca. 2000 Ma by $^{40}Ar/^{39}Ar$ single grain dating using a laser step-heating technique (Nam et al., 2000a). The orthogneiss has Nd model ages of 3.4–3.1 Ga and TIMS U–Pb zircon ages of 2.8–2.5 Ga (Lan et al., 2001).

3. Sample and zircon mineral descriptions

Zircons analyzed in this study were separated from three orthogneiss samples: HK22, RR03, and RR09. Zircons were mounted in epoxy-resin disks with several zircon-standard grains, and polished until they were exposed through their mid-grain sections, using 0.25 μm diamond paste. The standard and unknown-age zircons were imaged using a Scanning Electronic Microscope (SEM JSM-840) at Geological Institute, the University of Tokyo, in order to locate inclusion-free homogeneous regions suitable for SHRIMP analysis.

Sample HK22. The HK22 orthogneiss sample was collected from the Hung Khanh locality (21°35′49″N, 104°46′12″E; the same locality as the sample HK01 in Nam et al. (1998)) in the metamorphic belt south of the Day Nui Con Voi (Fig. 1(b)). Sample HK22 is coarse-grained and displays a gneissic texture. The main mineral constituents of the sample are quartz (10–15%), plagioclase (60–70%), K-feldspar (5–7%), hornblende (20–25%), biotite and epidote. Zircon and apatite are common accessory minerals.

HK22 zircons were concentrated by crushing, sieving, mineral separation with an isodynamic separator and heavy-liquids, and hand-picking under a binocular microscope. Zircons are brown, and range from 0.1 to 0.5 mm in length (Fig. 2). Large grains (0.25–0.5 mm) commonly have rounded ends, whereas small lighter-color grains are more euhedral (Fig. 2), suggesting that the zircon population represents different generations.

Figs. 3 and 4 show representative cathodoluminescence images of HK22 zircons (taken after SHRIMP analysis), in which three types of zoning patterns can be seen: (a) euhedral structured cores surrounded by an outer-core and a large homogeneous rim (Fig. 3(a)), (b) large structureless core and a narrow rim (Fig. 4(a) and (b)), and (c) homogeneous from the center to outer part of grain (Fig. 4(c) and (d)). Among 18 grains analyzed in this study, five grains have type (a), 10 grains display type (b), and three small grains have type (c) features. It is likely that these different zoning patterns correspond to different generations of zircons in the sample. As suggested below, the core of type (a) was from original igneous zircon, whereas types (b) and (c) are metamorphic generations. SHRIMP U–Pb

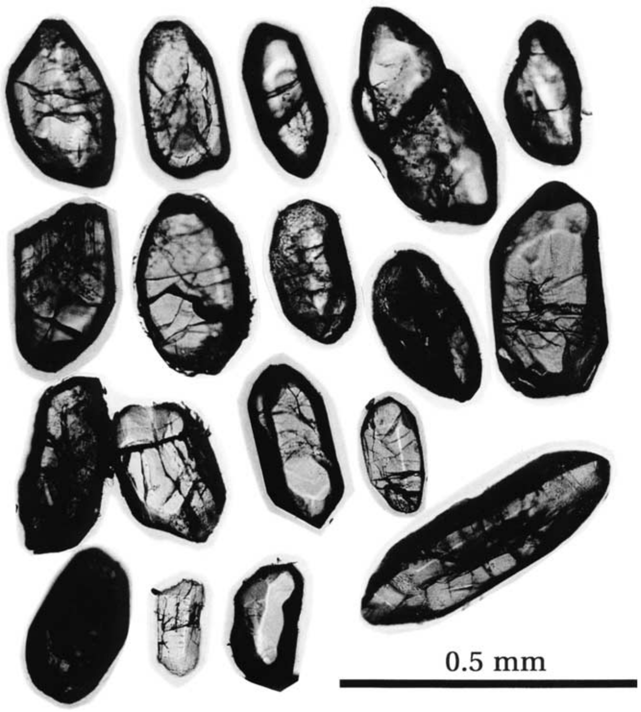

Fig. 2. Photographs of zircon from sample HK22 under transmitted light. Large grains are commonly brown and have rounded ends, whereas small grains are lighter and have subhedral to euhedral crystal shapes. Grains are arranged in order from left to right and from top to bottom as their numbers shown in Table 1 (note that there is no grain 17). Scale bar is 0.5 mm.

analyses have been performed on cores, outer-cores and overgrowth rims of zircons.

Samples RR03 and RR09. Two samples RR03 (21°37′17″N, 104°46′58″E) and RR09 (21°33′45″N, 104°45′32″E), both from the orthogneiss complex (CaVinh Complex) and close to our sample HK22 locality (Fig. 1(c)), were studied by Lan et al. (2001), who have reported TIMS U–Pb upper-intercept ages of around 2.83 Ga for zircons in these samples. Zircon separates RR03 and RR09 used in this study were provided by Sun-Lin Chung who is a co-author of Lan et al. (2001). Most zircons from RR03 and RR09 have rounded ends, are 0.2–0.3 mm in length, and are structureless in their SEM backscattered images. SHRIMP U–Pb analyses have been performed on cores and rims of zircons that showed internal zoning, and performed only on cores for the others.

4. Analytical methods and results

We used standard zircons SL13 and Quartz–Gabbro–Norite-Gneiss (QGNG). Standard SL13 is the well-known Sri Lanka 572 Ma megacryst extensively used by the Australian National University SHRIMP group as a U/Pb and abundance calibration standard (Roddick and van Breemen, 1994; Claoué-Long et al., 1995; Williams, 1998), and QGNG is a new multi-crystal zircon standard from a QGNG from Cape Donnington, Eyre Peninsula, South Australia whose TIMS U/Pb age is 1850 ± 2 Ma (2σ) (Fanning, personal communication, 1997). After polishing, the mount was coated with a thin gold film to prevent charging of the sample surface by the primary ion beam.

Before analysis, the sample surface was rastered for 2 min in order to clean up the surface of the grain from possible contaminants. A 2.5-nA mass-filtered O_2^- primary

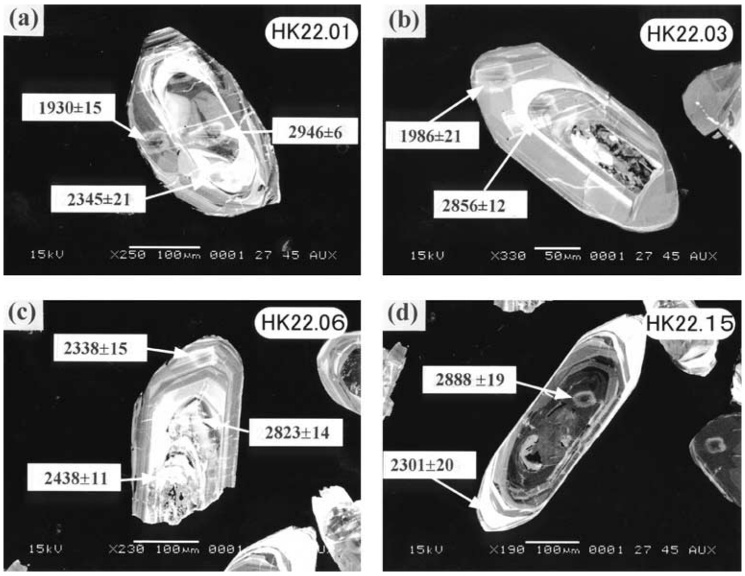

Fig. 3. Cathodoluminescence images of Late Archean (~2.9 Ga) zircons from the orthogneiss complex (sample HK22), northern Viet Nam. Old igneous cores show euhedral zoning. (a) A grain (HK22.01) with an igneous core (2946 ± 6 Ma), surrounded by two metamorphic zircon overgrowths: outer-core (2345 ± 21 Ma) and rim (1930 ± 15 Ma). (b) A grain (HK22.03) has a 1986 ± 21 Ma rim overgrown on its 2856 ± 12 Ma core, whereas two grains (HK22.06 in (c) and HK22.15 in (d)) show 2338–2301 Ma rims on old igneous cores of 2823–2888 Ma. Three zircon generations of ~2.9, ~2.4 and ~2.0 Ga are strongly suggested. Positions of spots of SHRIMP U–Pb analyses (small ovals) and their $^{207}Pb^*–^{206}Pb^*$ ages (in Ma) are shown. Scale bars are 100 μm.

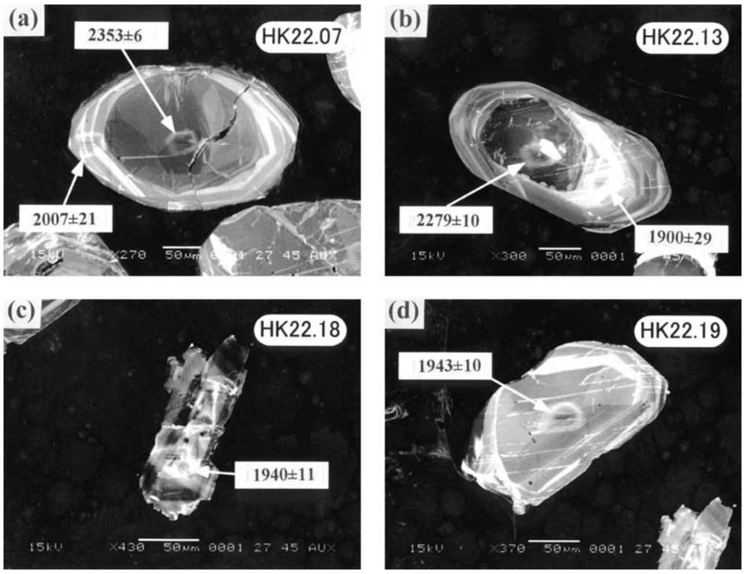

Fig. 4. Representative cathodoluminescence images of two younger (~2.36 and ~1.96 Ga) generations of zircons from the orthogneiss complex (sample HK22) northern Viet Nam. Two top grains HK22.07 (a) and HK22.13 (b) are metamorphic zircons with large structureless cores (2353 ± 6 and 2279 ± 10 Ma) and a narrow overgrowth rim (2007 ± 21 and 1900 ± 29 Ma). The two bottom grains HK22.18 (c) and HK22.19 (d) are small, new metamorphic zircons dated at 1940 ± 11 and 1943 ± 10 Ma, respectively. Positions of spots of SHRIMP U–Pb analyses and their $^{207}Pb^*-^{206}Pb^*$ ages (in Ma) are shown. Scale bars are 50 μm.

beam was focused to sputter a 20-μm-diameter area with positive ions extracted. The magnet was cyclically peak-stepped through a series of mass numbers ranging from mass 196 for $^{90}Zr_2^{16}O^+$ to mass 254 for $^{238}U^{16}O^+$, including the background at mass number 204.1, and Pb isotopic mass numbers at 204, 206, 207, and 208, and the atomic U peak at the number 238 and $^{232}Th^{16}O$ peak at number 248. The $^{206}Pb/^{238}U$ ratios in the samples were calibrated using an empirical relationship between $^{206}Pb^+/^{238}U^+$ and $^{238}U^{16}O^+/^{238}U^+$ ratios in standard zircons (Claoué-Long et al., 1995; Sano et al., 2000), and the $^{232}Th/^{238}U$ ratios were calibrated using the experimental equation of $^{232}Th/^{238}U = (0.03446(UO^+/U^+) + 0.868)(ThO^+/UO^+)$ (Williams et al., 1996). Subtraction of common Pb from measured Pb is required to estimate an accurate age. In this study, the measured $^{204}Pb/^{206}Pb$ ratio in each grain was used for the correction of common Pb (Compston et al., 1984). Experimental details are given elsewhere (Sano et al., 1999, 2000).

Table 1 lists zircon data for orthogneiss HK22. Fig. 5(a) shows a Tera-Wasserburg U–Pb zircon concordia diagram for the 36 analyses listed in Table 1. Most SHRIMP analyses of the zircon grains give near-concordant ages within experimental errors (Table 1; Fig. 5(a)). They could be classified into three main age groups as shown in a histogram-plot (Fig. 6). The oldest group consists of four analyses on zircon cores (HK22.01.1, HK22.03.1, HK22.06.1, and HK22.15.1 in Table 1; Figs. 3 and 5(a)), three of which have concordant and near-concordant ages, giving a weighted mean value of 2913 ± 10 Ma (2.9 Ga). The weighted mean value and its error were calculated for $^{207}Pb^*-^{206}Pb^*$ age data in Table 1, by using the following equations:

$$\bar{X} = \frac{\sum\left(\frac{x_i}{\Delta x_i^2}\right)}{\sum\left(\frac{1}{\Delta x_i^2}\right)}$$

and

$$\overline{\Delta X} = \sqrt{\frac{1}{\sum\left(\frac{1}{\Delta x_i^2}\right)}},$$

where $\bar{X} \pm \overline{\Delta X}$ are the weighted mean and its error, and $x_i \pm \Delta x_i$ are the data and their error sequences (Yoshizawa, 1989). The second group is composed of 21 analyses with a weighted mean age of 2362 ± 32 Ma (2.36 Ga), and the youngest group has a weighted mean age of 1964 ± 23 Ma (1.96 Ga). The weighted mean values were calculated using 15 and 9 concordant and near-concordant ages for the second and youngest group, respectively, and the age error is at a two-sigma confidence level. Some analyses from the two latter groups appear to be discordant (<80% confidence) (Table 1; Fig. 5(a)). Regression of the discordant ages yields a lower-intercept at 585 ± 260 and 567 ± 180 Ma (two-sigma level) for the two groups of 2.36 and 1.96 Ga, respectively.

Table 2 shows SHRIMP U–Th–Pb analytical data for 12 zircon grains from sample RR03 and 10 grains from sample RR09. Fig. 5(b) and (c) are Tera-Wasserburg U–Pb zircon concordia diagrams for the analytical data of the two samples. Both samples RR03 and RR09 show almost all data points clustered around 2.8 Ga on the concordia diagrams (Fig. 5(b) and (c)), and yield weighted mean ages of 2835 ± 6 and 2843 ± 8 Ma for their zircon

Table 1
SHRIMP U–Th–Pb analyses of zircons from orthogneiss sample HK22, south of the Day Nui Con Voi in northern Viet Nam

Sample/labels	U (ppm)	Th (ppm)	$^{204}Pb/^{206}Pb$	$^{207}Pb/^{206}Pb$	$^{208}Pb/^{206}Pb$	$^{238}U/^{206}Pb$	$^{232}Th/^{238}U$	$^{238}U-^{206}Pb^*$ age (Ma)	$^{207}Pb^*-^{206}Pb^*$ age (Ma)
HK22.01.1	148	1	0.000036 ± 0.000007	0.2158 ± 0.0008	0.0042 ± 0.0002	1.892 ± 0.146	0.0092 ± 0.0003	2734 ± 172	2946 ± 6
HK22.01.1*	36	16	0.000065 ± 0.000046	0.1508 ± 0.0017	0.1300 ± 0.0027	2.391 ± 0.118	0.4681 ± 0.0152	2251 ± 94	2345 ± 21
HK22.01.2	128	20	0.000056 ± 0.000015	0.1190 ± 0.0010	0.0450 ± 0.0007	3.030 ± 0.214	0.1581 ± 0.0047	1837 ± 113	1930 ± 15
HK22.02.1	266	39	0.000021 ± 0.000005	0.1465 ± 0.0019	0.0425 ± 0.0007	3.216 ± 0.266	0.1499 ± 0.0059	1745 ± 127	2302 ± 23
HK22.02.2	228	28	0.000043 ± 0.000043	0.1340 ± 0.0040	0.0381 ± 0.0016	2.426 ± 0.302	0.1276 ± 0.0083	2224 ± 234	2143 ± 52
HK22.03.1	115	57	0.000015 ± 0.000004	0.2039 ± 0.0015	0.1344 ± 0.0012	1.908 ± 0.155	0.5119 ± 0.0186	2717 ± 180	2856 ± 12
HK22.03.2	76	3	0.000035 ± 0.000010	0.1225 ± 0.0014	0.0127 ± 0.0007	2.671 ± 0.050	0.0422 ± 0.0008	2049 ± 33	1986 ± 21
HK22.04.1	233	45	0.000108 ± 0.000021	0.1407 ± 0.0014	0.0524 ± 0.0009	4.528 ± 0.273	0.1961 ± 0.0061	1284 ± 70	2218 ± 17
HK22.04.1*	24	12	0.000053 ± 0.000054	0.1551 ± 0.0018	0.1438 ± 0.0027	2.249 ± 0.145	0.5108 ± 0.0157	2370 ± 128	2396 ± 22
HK22.04.2	163	28	0.000269 ± 0.000031	0.1212 ± 0.0015	0.0608 ± 0.0024	3.099 ± 0.148	0.1738 ± 0.0035	1796 ± 75	1920 ± 24
HK22.05.1	28	19	0.000008 ± 0.000009	0.1453 ± 0.0019	0.2017 ± 0.0031	2.353 ± 0.086	0.6808 ± 0.0115	2283 ± 70	2290 ± 22
HK22.05.2	138	42	0.000016 ± 0.000010	0.1272 ± 0.0013	0.0865 ± 0.0035	2.668 ± 0.064	0.3127 ± 0.0103	2051 ± 42	2056 ± 18
HK22.06.1	76	28	0.000021 ± 0.000014	0.1998 ± 0.0017	0.1019 ± 0.0011	1.887 ± 0.051	0.3743 ± 0.0063	2740 ± 61	2823 ± 14
HK22.06.1*	78	51	0.000012 ± 0.000010	0.1585 ± 0.0010	0.1828 ± 0.0018	2.092 ± 0.093	0.6662 ± 0.0123	2518 ± 93	2438 ± 11
HK22.06.2	66	36	0.000050 ± 0.000012	0.1500 ± 0.0013	0.1526 ± 0.0014	2.299 ± 0.112	0.5646 ± 0.0123	2327 ± 95	2338 ± 15
HK22.07.1	319	99	0.000007 ± 0.000004	0.1507 ± 0.0005	0.0897 ± 0.0006	2.343 ± 0.129	0.3204 ± 0.0080	2291 ± 106	2353 ± 6
HK22.07.2	58	9	0.000228 ± 0.000060	0.1265 ± 0.0012	0.0536 ± 0.0014	2.922 ± 0.173	0.1559 ± 0.0042	1892 ± 97	2007 ± 21
HK22.08.1	293	79	0.000020 ± 0.000005	0.1512 ± 0.0006	0.0811 ± 0.0007	2.884 ± 0.146	0.2753 ± 0.0069	1919 ± 84	2357 ± 7
HK22.08.2	360	36	0.000039 ± 0.000012	0.1095 ± 0.0006	0.0311 ± 0.0005	4.309 ± 0.184	0.1032 ± 0.0018	1345 ± 52	1782 ± 10
HK22.09.1	313	55	0.000039 ± 0.000010	0.1579 ± 0.0024	0.0464 ± 0.0009	2.428 ± 0.088	0.1789 ± 0.0038	2223 ± 68	2428 ± 26
HK22.09.2	334	34	0.000163 ± 0.000026	0.1491 ± 0.0021	0.0389 ± 0.0015	3.869 ± 0.175	0.1035 ± 0.0021	1478 ± 60	2311 ± 25
HK22.10.1	281	98	0.000014 ± 0.000006	0.1468 ± 0.0013	0.0970 ± 0.0016	2.581 ± 0.122	0.3588 ± 0.0073	2110 ± 85	2307 ± 15
HK22.10.2	257	65	0.000043 ± 0.000011	0.1568 ± 0.0043	0.0674 ± 0.0027	2.310 ± 0.178	0.2601 ± 0.0119	2317 ± 150	2415 ± 46
HK22.11.1	59	39	0.000069 ± 0.000061	0.1704 ± 0.0028	0.1890 ± 0.0066	2.197 ± 0.107	0.6840 ± 0.0224	2416 ± 98	2553 ± 29
HK22.12.1	64	25	0.000068 ± 0.000082	0.1691 ± 0.0069	0.1259 ± 0.0063	2.958 ± 0.245	0.3936 ± 0.0169	1876 ± 135	2540 ± 68
HK22.13.1	109	48	0.000030 ± 0.000016	0.1447 ± 0.0008	0.1217 ± 0.0017	2.592 ± 0.124	0.4495 ± 0.0101	2103 ± 86	2279 ± 10
HK22.13.2	35	6	0.000065 ± 0.000036	0.1172 ± 0.0018	0.0465 ± 0.0014	3.109 ± 0.111	0.1664 ± 0.0054	1796 ± 56	1900 ± 29
HK22.14.1	287	104	0.000020 ± 0.000009	0.1570 ± 0.0018	0.0991 ± 0.0012	2.436 ± 0.122	0.3714 ± 0.0095	2217 ± 94	2421 ± 20
HK22.14.2	39	9	0.000006 ± 0.000005	0.1396 ± 0.0021	0.0677 ± 0.0022	2.778 ± 0.111	0.2305 ± 0.0073	1982 ± 68	2221 ± 26
HK22.15.1	265	27	0.000021 ± 0.000006	0.2080 ± 0.0024	0.0265 ± 0.0005	2.086 ± 0.094	0.1039 ± 0.0024	2524 ± 94	2888 ± 19
HK22.15.2	37	11	0.000122 ± 0.000033	0.1477 ± 0.0016	0.0877 ± 0.0020	2.579 ± 0.071	0.3136 ± 0.0053	2109 ± 49	2301 ± 20
HK22.16.1	265	9	0.000017 ± 0.000010	0.1383 ± 0.0008	0.0108 ± 0.0004	3.901 ± 0.186	0.0349 ± 0.0015	1471 ± 63	2204 ± 10
HK22.16.1*	101	10	0.000040 ± 0.000012	0.1180 ± 0.0009	0.0305 ± 0.0007	3.054 ± 0.137	0.1059 ± 0.0026	1825 ± 71	1918 ± 14
HK22.16.2	413	16	0.000033 ± 0.000015	0.1129 ± 0.0005	0.0119 ± 0.0003	4.170 ± 0.216	0.0405 ± 0.0010	1385 ± 65	1839 ± 9
HK22.18.1	203	61	0.000016 ± 0.000004	0.1191 ± 0.0008	0.0898 ± 0.0010	2.971 ± 0.173	0.3103 ± 0.0067	1870 ± 95	1940 ± 11
HK22.19.1	140	28	0.000020 ± 0.000010	0.1194 ± 0.0007	0.0600 ± 0.0008	3.218 ± 0.140	0.2081 ± 0.0042	1744 ± 67	1943 ± 10

First sub-numbers with sample name (example HK22.01) show each grain of zircon analyzed. Second sub-numbers, such as HK22.01.1 and HK22.01.2 indicate different pit positions on a single grain HK22.01; generally X.1 shows a core, X.1* is an outer-core and X.2 is a rim of the zircon. Note that there is a significant change of U concentration even in a single grain. Data corrected using ^{204}Pb. Errors assigned to the isotopic, elemental ratios and the radiogenic ages are one-sigma level.

$^{207}Pb^*-^{206}Pb^*$ ages (Fig. 5(b) and (c)). Three analyses give ages of 2.3–2.4 Ga (RR03.06.1, RR03.07.3, and RR09.07.2 in Table 2; Fig. 5(b) and (c)), and another two analyses yield ages of 2.0 Ga (RR03.01.1 and RR09.01.2 in Table 2; Fig. 5(b) and (c)).

5. Discussion

5.1. Three generations of zircon and Late Archean protolith age of the orthogneiss complex, northern Viet Nam

The combination of zoning patterns and their SHRIMP U–Pb dates shown in Figs. 3 and 4 indicates that there are three zircon generations in orthogneiss sample HK22. The first generation is represented by ~2.9 Ga cores (Fig. 3). The second generation includes ~2.36 Ga outer-cores (Fig. 3(a)) and ~2.36 Ga rims overgrown on ~2.9 Ga cores (Fig. 3(c) and (d)), and large structureless cores (Fig. 4(a) and (b)). The third generation is composed of ~1.96 Ga rims overgrown on the older generations (Figs. 3(a), (b) and 4(b)) and new grown small grains (Fig. 4(c) and (d)). It is well known that magmatic zircons are strongly zoned and have large crystal faces, whereas metamorphic zircons do not show well-developed internal zoning (Mezger and Krogstad, 1997). The oldest zircon cores in this study appear to be strongly zoned with likely euhedral internal crystal faces (Fig. 3). This leads to a suggestion that the first zircon generation was magmatic. The two later zircon generations have generally no structured zoning (Fig. 4),

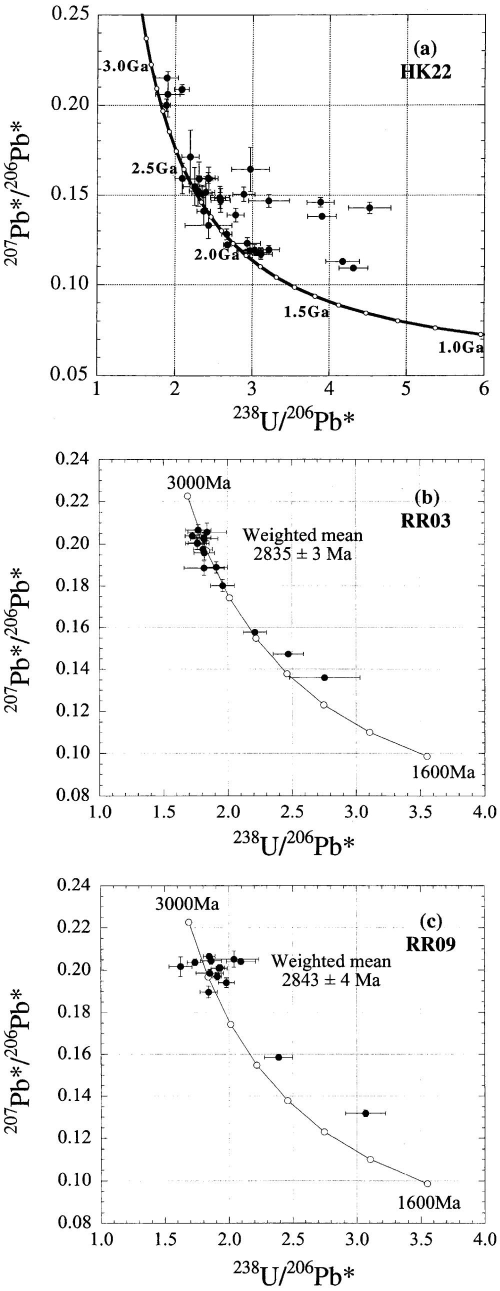

Fig. 5. Tera-Wasserburg U–Pb zircon concordia diagram for sample HK22 (a), RR03 (b) and RR09 (c) from the orthogneiss complex, northern Viet Nam. Error bars are shown at two-sigma level.

therefore, they perhaps were likely formed during high-grade tectono-metamorphic events (metamorphic growth). The youngest zircons commonly have a small size and sub-euhedral crystal shape (Fig. 2), and some of the second group shows an internal zoning structure (Fig. 3(c)), suggesting growth in the presence of melt; probably partial-melting during high-grade metamorphism.

Lan et al. (2001) reported TIMS U–Pb zircon upper-intercept ages of 2.83 Ga for samples RR03 and RR09. Our SHRIMP U–Pb dating of zircons from these samples shows that there are three age groups in the two samples. The old zircon group of 2.84 Ga ages was dominant (24 among 29 analyses), and is generally consistent with their TIMS dates. The second group includes three analyses of 2.3–2.4 Ga, and the third group shows ages of 2.0 Ga, as mentioned in Section 4 (Table 2; Fig. 5(b) and (c)). Since the RR03 and RR09 samples were less deformed than our HK22 sample, the old zircon population is dominant in these samples, and the two younger generations are less common. It is clear that there are three zircon generations in the orthogneiss complex (Fig. 6).

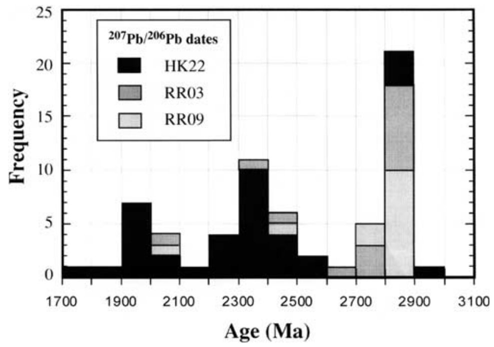

Fig. 6. Age ($^{207}Pb–^{206}Pb$) distributions for SHRIMP U–Pb zircon analyses of the orthogneiss complex, northern Viet Nam. Three age populations are identified. Note that two data points younger than 1900 Ma are from spots HK22.08.2 and HK22.16.2 on rims which appear discordant (Table 1).

From the above discussion, the apparent U–Pb ages of ca. 2.84–2.9 Ga obtained on several zircons are interpreted to be the magma-crystallization age of the orthogneiss. However, the 2.9 Ga old zoned cores were overgrown by the two younger zircon generations (2.36 Ga outer-cores, 2.36 and 1.96 Ga rims; Fig. 3), indicating that the cores have suffered as least two later high-grade thermal events. It has been recently proposed that the closure temperature for the zircon U–Pb system was greater than 850 °C (Claoué-Long et al., 1995; Lee et al., 1997; Mezger and Krogstad, 1997; Sano et al., 1999), although it was previously accepted to be ~750 °C (Mattinson, 1978). Lee et al. (1997) have estimated the closure temperature for the U–Th–Pb system in natural zircon to be greater than 900 °C. The zoned zircon could recrystallize during later high-grade metamorphism (Pidgeon, 1992; Mezger and Krogstad, 1997). Radiogenic Pb can be partially lost during recrystallization and other processes, including radiation damage, self-annealing and chemical reaction (Pidgeon, 1992; Mezger and Krogstad, 1997; Sano et al., 1999). Many zircons in this study have rounded ends (Fig. 2), consistent with recrystallization of zircons as a result of partial dissolution (Mezger and Krogstad, 1997). Therefore, the old age of 2.9 Ga could be interpreted as a minimum age for the protolith of the orthogneiss.

5.2. Thermal evolution of the orthogneiss complex

Since the 2.9 Ga old zircon cores in sample HK22 were overgrown by younger zircon rims of 2.36 and 1.96 Ga

Table 2
SHRIMP U–Th–Pb analyses of zircons from orthogneiss samples RR03 and RR09, south of the Day Nui Con Voi in northern Viet Nam

Sample/labels	U (ppm)	Th (ppm)	$^{204}Pb/^{206}Pb$	$^{207}Pb/^{206}Pb$	$^{208}Pb/^{206}Pb$	$^{238}U/^{206}Pb$	$^{232}Th/^{238}U$	$^{238}U-^{206}Pb^*$ age (Ma)	$^{207}Pb^*-^{206}Pb^*$ age (Ma)
RR03.01.1	1830	944	0.000009 ± 0.000002	0.1360 ± 0.0009	0.1492 ± 0.0015	2.755 ± 0.275	0.5290 ± 0.0239	1996 ± 171	2176 ± 11
RR03.03.1	97	44	0.000214 ± 0.000047	0.2028 ± 0.0028	0.1372 ± 0.0016	1.765 ± 0.092	0.4666 ± 0.0121	2894 ± 121	2828 ± 23
RR03.04.1	108	45	0.000010 ± 0.000009	0.2068 ± 0.0024	0.1174 ± 0.0017	1.771 ± 0.100	0.4327 ± 0.0129	2886 ± 131	2880 ± 19
RR03.05.1	58	35	0.000532 ± 0.000128	0.1953 ± 0.0019	0.1813 ± 0.0026	1.911 ± 0.086	0.6163 ± 0.0133	2713 ± 99	2733 ± 24
RR03.06.1	598	150	0.000005 ± 0.000003	0.1578 ± 0.0006	0.0709 ± 0.0005	2.210 ± 0.091	0.2566 ± 0.0048	2407 ± 83	2431 ± 7
RR03.07.1	230	62	0.000013 ± 0.000005	0.1960 ± 0.0032	0.0736 ± 0.0010	1.819 ± 0.079	0.2773 ± 0.0051	2825 ± 99	2792 ± 26
RR03.07.2	13	1	0.000042 ± 0.000113	0.1807 ± 0.0023	0.0289 ± 0.0016	1.960 ± 0.091	0.0927 ± 0.0039	2657 ± 102	2655 ± 26
RR03.07.3	941	379	0.000002 ± 0.000003	0.1472 ± 0.0008	0.1162 ± 0.0006	2.469 ± 0.119	0.4133 ± 0.0064	2193 ± 89	2314 ± 9
RR03.08.1	172	240	0.000096 ± 0.000018	0.2069 ± 0.0042	0.3930 ± 0.0116	1.840 ± 0.149	1.4337 ± 0.0744	2798 ± 184	2872 ± 33
RR03.09.1	277	197	0.000018 ± 0.000009	0.2040 ± 0.0007	0.1966 ± 0.0016	1.725 ± 0.056	0.7294 ± 0.0096	2947 ± 77	2857 ± 5
RR03.10.1	601	373	0.000007 ± 0.000002	0.1977 ± 0.0022	0.1718 ± 0.0037	1.809 ± 0.073	0.6377 ± 0.0114	2836 ± 92	2807 ± 18
RR03.10.2	10	1	0.000076 ± 0.000057	0.1896 ± 0.0033	0.0298 ± 0.0019	1.817 ± 0.156	0.1108 ± 0.0060	2827 ± 197	2731 ± 30
RR03.11.1	461	724	0.000244 ± 0.000020	0.2034 ± 0.0005	0.4349 ± 0.0024	1.764 ± 0.072	1.6110 ± 0.0327	2895 ± 96	2831 ± 5
RR03.12.1	101	124	0.000011 ± 0.000008	0.2026 ± 0.0011	0.3374 ± 0.0032	1.816 ± 0.106	1.2601 ± 0.0397	2828 ± 133	2847 ± 9
RR03.14.1	255	355	0.000004 ± 0.000003	0.2030 ± 0.0023	0.3889 ± 0.0020	1.816 ± 0.055	1.4283 ± 0.0135	2828 ± 70	2850 ± 18
RR09.01.1	96	136	0.000006 ± 0.000007	0.1898 ± 0.0027	0.3976 ± 0.0027	1.843 ± 0.067	1.4464 ± 0.0297	2795 ± 82	2740 ± 24
RR09.01.2	694	36	0.000001 ± 0.000002	0.1318 ± 0.0016	0.0145 ± 0.0003	3.069 ± 0.156	0.0534 ± 0.0016	1818 ± 81	2122 ± 21
RR09.02.1	190	104	0.000006 ± 0.000006	0.1972 ± 0.0018	0.1559 ± 0.0020	1.908 ± 0.034	0.5639 ± 0.0074	2717 ± 39	2802 ± 15
RR09.03.1	180	220	0.000017 ± 0.000006	0.2039 ± 0.0016	0.3389 ± 0.0037	1.737 ± 0.061	1.2547 ± 0.0168	2932 ± 83	2856 ± 13
RR09.03.2	112	83	0.000011 ± 0.000008	0.2019 ± 0.0046	0.2146 ± 0.0022	1.623 ± 0.090	0.7620 ± 0.0224	3094 ± 136	2840 ± 37
RR09.04.1	137	234	0.000007 ± 0.000005	0.2053 ± 0.0038	0.4832 ± 0.0064	2.041 ± 0.195	1.7544 ± 0.0833	2571 ± 203	2868 ± 30
RR09.05.1	105	77	0.000009 ± 0.000009	0.2010 ± 0.0014	0.2062 ± 0.0019	1.924 ± 0.062	0.7522 ± 0.0093	2699 ± 71	2834 ± 11
RR09.06.1	84	52	0.000003 ± 0.000007	0.2042 ± 0.0014	0.1640 ± 0.0016	2.094 ± 0.115	0.6323 ± 0.0159	2516 ± 114	2860 ± 11
RR09.07.1	80	101	0.000006 ± 0.000007	0.2046 ± 0.0016	0.3358 ± 0.0024	1.860 ± 0.083	1.2950 ± 0.0216	2774 ± 100	2862 ± 13
RR09.07.2	498	12	0.000018 ± 0.000008	0.1588 ± 0.0011	0.0067 ± 0.0002	2.388 ± 0.110	0.0248 ± 0.0008	2255 ± 87	2441 ± 11
RR09.08.1	93	92	0.000018 ± 0.000010	0.2068 ± 0.0012	0.2667 ± 0.0027	1.847 ± 0.047	1.0076 ± 0.0159	2790 ± 57	2879 ± 9
RR09.09.1	519	459	0.000021 ± 0.000005	0.1988 ± 0.0018	0.2513 ± 0.0014	1.851 ± 0.106	0.9069 ± 0.0252	2784 ± 130	2814 ± 15
RR09.09.2	304	94	0.000006 ± 0.000005	0.2012 ± 0.0017	0.0902 ± 0.0014	1.932 ± 0.032	0.3177 ± 0.0023	2689 ± 36	2835 ± 14
RR09.10.1	73	99	0.000013 ± 0.000031	0.1943 ± 0.0022	0.3814 ± 0.0051	1.980 ± 0.062	1.3927 ± 0.0260	2636 ± 68	2777 ± 19

Data corrected using ^{204}Pb. Errors assigned to the isotopic, elemental ratios and the radiogenic ages are one-sigma level.

(Fig. 3), and the two younger zircon generations commonly have no structured zoning (Fig. 4) as mentioned earlier, it is suggested that these younger zircons most likely grew during later high-grade metamorphic episodes. High-grade events could be accompanied by juvenile magma generation from depleted mantle sources or/and crustal melts. Therefore, zircons grown during these events, in the presence of melts, could appear to have internal structured zoning (Fig. 3(c)), and could be regarded as magmatic grains. In the case of the metamorphic belt south of the Day Nui Con Voi, the rock assemblage of orthogneisses and migmatites suggests most likely the partial-melting of existing Late Archean crust rather than a pure mantle source, at least for the 1.96 Ga event. Nevertheless, the SRHIMP U–Pb zircon ages of 2.36 and 1.96 Ga dated the timing of two high-grade metamorphic events that have strongly affected the protolith and formed the orthogneisses. Synkinematic hornblendes from an orthogneiss sample (HK01) collected at the same outcrop as HK22, and hornblendes from an amphibolite lens (HK05) within the metamorphic belt (Fig. 1(c)) have given K/Ar ages of 1700 and 2000 Ma, respectively (Nam et al., 1998). The same hornblendes were then dated by $^{40}Ar/^{39}Ar$ laser step-heating techniques on single grains. Three grains of HK01 yielded plateau ages of 1873 ± 13, 1977 ± 19 and 2089 ± 14 Ma, and two grains of HK05 yielded 2044 ± 21 and 2056 ± 14 Ma plateau ages (Nam et al., 2000a). These $^{40}Ar/^{39}Ar$ ages indicate the cooling ages of the hornblendes, which grew during an Early Proterozoic tectonothermal event. The youngest zircon age of 1.96 Ga obtained in the present study is generally consistent with these $^{40}Ar/^{39}Ar$ ages, although it is unclear why some hornblende grains (especially those from amphibolite HK05) gave apparent plateau ages slightly older than the zircon age. There is a possibility that excess argon components existed in the rocks, causing the older dates and resulting in the plateau age variation.

Fig. 7 shows two possible thermal histories for the orthogneiss complex constrained by using the present SHRIMP U–Pb zircon ages and other available geochronological data. From Fig. 7, it is inferred that the protolith of the orthogneiss complex south of the Day Nui Con Voi (northern Viet Nam) had formed in Archean times at ~2.9 Ga. However, it is unclear whether the magmatism in the complex continued from 2.9 (SHRIMP U–Pb zircon age

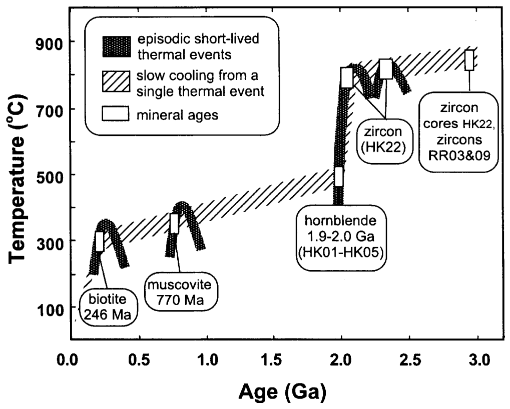

Fig. 7. Two possible thermal histories for the orthogneiss complex, northern Viet Nam. Cooling ages of biotite (after Tri (1977)), and of muscovite (from Nam et al. (2000b)) corresponding to the Indosinian (210–250 Ma) and Jinning (0.8–1.0 Ga) Orogenies, respectively. See text for further discussion.

for the sample HK22) to 2.84 Ga (SHRIMP U–Pb dates for RR03 and RR09 zircon samples), or represents more than one episode. The Archean protolith then underwent two high-grade tectonothermal events that occurred during Early Proterozoic times (2.36 and 1.96 Ga). Bodet and Schärer (2000) have shown that there were two Early Proterozoic events at 2.3–2.2 and 2.0–1.9 Ga in the SE-Asian continent, suggested from U–Pb zircon and baddeleyite ages. Our two Early Proterozoic tectonothermal events are consistent with their data. Post-Early Proterozoic events that affected the orthogneiss complex likely occurred at ca. 770 Ma (K–Ar muscovite age; Nam et al., 2000b) during the Late Proterozoic (0.8–1.0 Ga) Jinning Orogeny, and at ca. 246 Ma (K–Ar biotite age; Tri, 1977) during the Triassic (210–250 Ma) Indosinian Orogeny. U–Pb zircon upper-intercept ages of 838 ± 45 Ma recently reported for one gneiss sample from the Day Nui Con Voi (Lan et al., 2001), U–Pb zircon ages of 245 Ma (sample VN38 of Carter et al. (2001)) and $^{40}Ar/^{39}Ar$ mica ages of 200–236 Ma in the northern Viet Nam region (Maluski et al. 2001; Fig. 1(b)) could be attributed to the two later events. Since the orthogneiss complex does not appear to be significantly affected by the Tertiary tectonothermal event, it is argued that the Tertiary high-grade event in this region was likely restricted to the Red River shear zone.

The orthogneiss complex may instead record a single thermal event during Early Proterozoic times. In this scenario, Early Proterozoic magmatic episodes lasted from 2.36 to 1.96 Ga to form the protolith of the complex. The ~2.9 Ga zircon cores (HK22) and 2.84 Ga zircons (RR03 and RR09) are then interpreted to be inherited components from complex source lithologies melted at that time (S-type granitic rocks). Following this suggestion, the Archean inherited components should be negligible in term of the total budget of the orthogneiss complex rocks, and they may show a wide range of ages. However, as mentioned in Section 5.1, recent Sm–Nd isotopic and zircon dating studies of the complex showed Nd T_{DM} ages of 3.4–3.1 Ga and TIMS U–Pb zircon upper-intercept ages of 2.83 Ga (Lan et al., 2001), while new SHRIMP U–Pb zircon dating of the complex in this study yielded 2.84 Ga ages for samples RR03 and RR09. The younger TIMS zircon upper-intercept ages could be explained in term of ‘mixed ages’ resulting from some multi-overgrowth zircons. These data strongly support Archean ages for the orthogneiss complex rather than for inherited components. Therefore, the single thermal scenario is unlikely, and the multi-event history as mentioned earlier and illustrated in Fig. 7 is the most plausible scenario.

5.3. Implication for the crustal evolution of northern Viet Nam and the South China Block

Lan et al. (2000), using Nd isotopic evolution models to link the I-type granitic rocks of the Mid-Proterozoic Posen complex in northern Viet Nam with that of the Yangtze craton (South China Block), argued that northern Viet Nam was formed during Proterozoic time. Bodet and Schärer (2000) dated 235 single zircon and baddeleyite grains from large rivers in the Indochina continent by the U–Pb chronometer, and analyzed for Hf isotopes. Their analyses define age groups all younger than 2.5 Ga, and reveal five different Proterozoic crustal growth events occurring at ~2.5, 2.3–2.2, 2.0–1.9, 1.2–1.1 Ga (Grenvillian Orogeny), and 0.8 Ga (Jinning Orogeny) for the SE-Asian region. Our two younger SHRIMP U–Pb zircon age groups of 2.36 and 1.96 Ga are generally consistent with their data. However, the 2.9 Ga SHRIMP U–Pb zircon age of HK22, 2.84 Ga SHRIMP U–Pb zircon ages for samples RR03 and RR09 in this study, TIMS U–Pb ages of 2.83–2.54 Ga for single zircon grains and Nd model ages of 3.42–3.12 Ga reported by Lan et al. (2001) for the orthogneiss complex provide evidence for the presence of Archean rocks in Indochina and strongly indicate that the crustal evolution of northern Viet Nam began in Late Archean times. The argument by Bodet and Schärer (2000) that no crust-forming event older than 2.5 Ga can be identified for the SE-Asian region, therefore, is not correct.

Zircon ages of 2.9 Ga have been reported for the Kongling gneisses from the Huangling area of the Yangtze craton, South China Block (Ames et al., 1996; Fig. 1(a)). This led Chen and Jahn (1998) to suggest that the presence of Archean rocks in the Yangtze craton is likely limited to the northern margin of the craton. Chen and Jahn (1998) have therefore argued that the main crust-forming events for the Yangtze craton took place in the Proterozoic based on Nd model ages. An Archean protolith age is now clearly identified, and two Early Proterozoic high-grade tectonothermal events have been discerned for the orthogneiss complex in northern Viet Nam by SHRIMP U–Pb zircon dates. Together with other available data (Lan et al. 2001; Bodet and Schärer, 2000), it is suggested that the crustal nucleus of the South China Block, including northern Viet Nam, formed in the Late Archean and was affected by at least two Early Proterozoic (2.36–2.2 and 2.0–1.96 Ga) tectonothermal events.

6. Conclusions

1. Three zircon generations in the orthogneiss complex south of the Red River shear zone in Viet Nam give SHRIMP U–Pb ages of ~2.9, 2.36 and 1.96 Ga. The ~2.9 Ga zircons provide a minimum age for the protolith of the complex. Two younger zircon generations of 2.36 and 1.96 Ga date the timing of two high-grade tectonothermal events that have strongly affected the Archean (~2.9 Ga) protolith.
2. The orthogneiss complex south of the Red River shear zone in Viet Nam has recorded a multi-event history revealed from geochronological data, including primary magma-crystallization at ~2.9 Ga and two Early Proterozoic (2.36 and 1.96 Ga) high-grade tectonothermal events. In addition, Late Proterozoic (0.8–1.0 Ga) and Indosinian (210–250 Ma) events have also been determined.
3. The ~2.9 Ga protolith age of the orthogneiss complex confirms the presence of Archean rocks in Indochina, and indicates that the crustal evolution of northern Viet Nam started as early as Late Archean time.

Acknowledgments

The authors thank Sun-Lin Chung for providing RR03 and RR09 zircon separates, Y. Hiroi and H. Yoshida for cathodoluminescence and SEM assistance. The authors also thank R. Lacassin, K. Mezger for their comments and suggestions on an earlier draft. Careful reviews by S. Wilde and H. Maluski improved the manuscript. A post-doctoral fellowship and a Grant-in Aid (ID No. P98376) from the Ministry of Education, Science, Sport and Culture, Government of Japan (Monbusho) and a visiting scientist position from the University of Tokyo to TNN is gratefully acknowledged. This work was also financially supported in part by Natural Science Council of Viet Nam. This is a contribution of the Hiroshima SHRIMP laboratory.

References

Ames, L., Zhou, G.Z., Xiong, B.C., 1996. Geochronology and isotopic character of ultrahigh-pressure metamorphism with implications for collision of Sino-Korean and Yangtze cratons, central China. Tectonics 15, 472–489.

Bodet, F., Schärer, U., 2000. Evolution of the SE-Asian continent from U–Pb and Hf isotopes in single grains of zircon and baddeleyite from large rivers. Geochimica et Cosmochimica Acta 64, 2067–2091.

Carter, A., Roques, D., Bristow, C., Kinny, P., 2001. Understanding Mesozoic accretion in Southeast Asia: significance of Triassic thermotectonism (Indosinian Orogeny) in Viet Nam. Geology 29, 211–214.

Chen, J.F., Jahn, B.M., 1998. Crustal evolution of southeastern China: Nd and Sr isotopic evidence. Tectonophysics 284, 101–133.

Claoué-Long, J.C., Compston, W., Robert, J., Fanning, C.M., 1995. Two Carboniferous ages: a comparison of SHRIMP zircon dating with conventional zircon ages and $^{40}Ar/^{39}Ar$ analysis. Geochronology, Time Scales and Global Stratigraphic Correlation, Society for Sedimentary Geology Special Publication, 4., pp. 3–21.

Compston, W., Williams, I.S., Meyer, C., 1984. U–Pb geochronology of zircons from lunar breccia 73217 using a sensitive high mass-resolution ion microprobe. Journal of Geophysical Research 89 (Supllement), B525–B534.

Hai, T.Q., 1986. Precambrian Stratigraphy of Indochina, Geology of Kampuchea, Laos and Viet Nam, Science Publisher, Hanoi, pp. 20–30; in Viet Namese with English Abstract.

Harrison, T.M., Leloup, P.H., Ryerson, F.J., Tapponnier, P., Lacassin, R., Wenji, C., 1996. Diachronous initiation of transtention along the Ailao Shan–Red River shear zone, Yunnan and Viet Nam. In: Yin, A., Harrison, T.M. (Eds.), The Tectonic Evolution of Asia, Cambridge University Press, New York, pp. 208–226.

Hutchison, C.S., 1989. Geological Evolution of South-East Asia, Oxford Science Publications, Oxford, p. 368.

Jolivet, L., Maluski, H., Beyssac, O., Goffe, B., Lepvrier, C., Thi, P.T., Vuong, N.V., 1999. Oligocene–Miocene Bu Khang extensional gneiss dome in Viet Nam: geodynamic implications. Geology 27, 67–70.

Lan, C.Y., Chung, S.L., Shen, J.J.S., Lo, C.H., Wang, P.L., Hoa, T.T., Thanh, H.H., Mertzman, S.A., 2000. Geochemical and Sr–Nd isotopic characteristics of granitic rocks from northern Viet Nam. Journal of Asian Earth Sciences 18, 267–280.

Lan, C.Y., Chung, S.L., Lo, C.H., Lee, T.Y., Wang, P.L., Li, H., Toan, D.V., 2001. First evidence for Archean continental crust in northern Viet Nam and its implications for crustal and tectonic evolution in Southeast Asia. Geology 19, 219–222.

Lee, J.K.W., Williams, I.S., Ellis, D.J., 1997. Pb, U and Th diffusion in natural zircon. Nature 390, 159–162.

Leloup, P.H., Lacassin, R., Tapponnier, P., Schärer, U., Dailai, Z., Xiaohan, L., Liangshang, Z., Shaocheng, J., Trinh, P.T., 1995. The Ailao Shan–Red River shear zone (Yunnan, China), Tertiary transform boundary of Indochina. Tectonophysics 251, 3–84.

Lepvrier, C., Maluski, H., Vuong, N.V., Roques, D., Axente, V., Rangin, C., 1997. $^{40}Ar/^{39}Ar$ Indosinian age of NW-trending dextral shear zones within the Truong Son belt (Viet Nam): Cretaceous to Cenozoic overprinting. Tectonophysics 283, 105–127.

Maluski, H., Lepvrier, C., Roques, D., Vuong, N.V., Quynh, P.V., Rangin, C., 1995. $^{40}Ar–^{39}Ar$ Ages in the Da Nang–Dai Loc Plutono-metamorphic Complex (Central Viet Nam). Overprinting Process of Cenozoic over Indosinian Thermotectonic Episodes, International Symposium On Cenozoic Evolution of the Indochina Peninsula (abstract), Hanoi, 25–29 April, p. 65.

Maluski, H., Lepvrier, C., Vuong, N.V., Wemmer, K., 1997. Overprinting of Indosinian Terranes in the Truong Son Belt (Central to Northern Viet Nam). EUG, 491Abstract volume.

Maluski, H., Lepvrier, C., Jolivet, L., Carter, A., Roques, D., Beyssac, O., Tang, T.T., Thang, N.D., Avigad, D., 2001. Ar–Ar and fission-track ages in the Song Chay Massif: Early Triassic and Cenozoic tectonics in northern Viet Nam. Journal of Asian Earth Sciences 19, 233–248.

Mattinson, J.M., 1978. Age, origins and thermal histories of some plutonic rocks from the Salinian Block of California. Contributions to Mineralogy and Petrology 67, 233–245.

Mezger, K., Krogstad, E.J., 1997. Interpretation of discordant U–Pb ages: an evaluation. Journal of Metamorphic Geology 15, 127–140.and references therein.

Nam, T.N., 1998. Thermotectonic events from Early Proterozoic to Miocene in the Indochina craton: implication of K–Ar ages in Viet Nam. Journal of Asian Earth Sciences 16, 475–484.

Nam, T.N., Toriumi, M., Itaya, T., 1998. P–T–t paths and post-metamorphic exhumation of the Day Nui Con Voi shear zone in Viet Nam. Tectonophysics 290, 299–318.

Nam, T.N., Hyodo, H., Itaya, T., Matsuda, T., 2000a. Early Proterozoic tectonothermal event south of the Red River shear zone in Viet Nam: first evidence from $^{40}Ar/^{39}Ar$ dating of single grain hornblendes. Journal of Sciences (VNU) T.XVI (2), 26–34.

Nam, T.N., Toriumi, M., Itaya, T., Okada, T., Long, T.V., Kiem, D.D., 2000b. Tectonothermal events in Indochinese crystalline basement: evidence from geochronological data. Eos Transactions, AGU 81 (22), 190.

Nam, T.N., Sano, Y., Terada, K., Toriumi, M., Quynh, P.V., Dung, L.T., 2001. First SHRIMP U–Pb zircon dating of granulites from the Kontum massif (Viet Nam) and tectonothermal implications. Journal of Asian Earth Sciences 19, 77–84.

Pidgeon, R.T., 1992. Recrystallization of oscillatory zoned zircon: some geochronological and petrological implications. Contributions to Mineralogy and Petrology 110, 463–472.

Roddick, J.C., van Breemen, O., 1994. U–Pb dating: a comparison of ion microprobe and single grain conventional analyses. Radiogenic Age and Isotope Studies: Report 8, Geological Survey of Canada Current Research, pp. 1–9.

Sano, Y., Terada, K., Hidaka, H., Yokoyama, K., Nutman, A.P., 1999. Paleoproterozoic thermal events recorded in the ~4.0 Ga Acasta gneiss, Canada: evidence from SHRIMP U–Pb dating of apatite and zircon. Geochimica and Cosmochimica Acta 63, 899–905.

Sano, Y., Hidaka, H., Terada, K., Shimizu, H., Suzuki, M., 2000. Ion microprobe U–Pb zircon geochronology of Hida gneiss: finding of the oldest minerals in Japan. Geochemical Journal 34, 135–153.

Schärer, U., Tapponnier, P., Lacassin, R., Leloup, P.H., Zhong, D., Ji, S., 1990. Intraplate tectonics in Asia: a precise age for large-scale Miocene movement along the Ailao Shan–Red River fault zone, China. Earth and Planetary Science Letters 97, 65–77.

Schärer, U., Lian-Sheng, Z., Tapponnier, P., 1994. Duration of strike-slip movements in large shear zone: the Red River belt, China. Earth and Planetary Science Letters 126, 379–397.

Tapponnier, P., Peltzer, G., Armijo, R., 1986. On the mechanics of the collision between India and Asia. Special Publications of Geological Society of London 19, 115–157.

Tapponnier, P., Lacassin, R., Leloup, P.H., Schärer, U., Zhong, D., Wu, H., Liu, X., Ji, S., Zhang, L., Zhong, J., 1990. The Ailao Shan–Red River metamorphic belt: Tertiary left-lateral shear between Sundaland and South China. Nature 343, 431–437.and references therein.

Tri, T.V. (Ed.), 1977. Geology of Viet Nam: The Northern Part, Science Publisher, Hanoi, p. 354, in Viet Namese.

Wang, P.-L., Lo, C.-H., Li, T.-Y., Chung, S.-L., Lan, C.-Y., Yem, N.T., 1998. Thermochronological evidence for the movement of the Ailao Shan–Red River shear zone: a perspective from Viet Nam. Geology 26, 887–890.

Wang, P.-L., Lo, C.-H., Li, T.-Y., Chung, S.-L., Lee, T.-Y., Lan, C.-Y., Thang, T.V., 2000. Onset timing of left-lateral movement along the Ailao Shan–Red River shear zone: $^{40}Ar/^{39}Ar$ dating constraint from Nam Dinh Area, northeastern Viet Nam. Journal of Asian Earth Sciences 18, 281–292.

Williams, I.S., 1998. U–Pb–Th geochronology by ion microprobe. In: McKibben, M.A., Shanks, W.C. III, Ridley, W.I. (Eds.), Applications of Microanalytical Techniques to Understanding Mineralizing Processes, Reviews in Economic Geology 7, pp. 1–35.

Williams, I.S., Buick, I.S., Cartwright, I., 1996. An extended episode of early Mesoproterozoic metamorphic fluid flow in Reynolds Range, central Australia. Journal of Metamorphic Geology 14, 29–47.

Yoshizawa, Y., 1989. New Theory of Errors, Kyoritsu Shuppan Co. Ltd, p. 128; in Japanese.

Zhang, L.S., Schärer, U., 1999. Age and origin of magmatism along the Cenozoic Red River shear belt, China. Contributions to Mineralogy and Petrology 134, 67–85.